

# Excited electron production at the SPPC-based ep colliders via contact interactions

A. Caliskan\*

*Gümüşhane University, Faculty of Engineering and Natural Sciences,  
Department of Physics Engineering, 29100, Gümüşhane, Türkiye*

## Abstract

If a linear electron accelerator is installed into the SPPC (Super Proton-Proton Collider) complex, ep collision options will be available in addition to pp collisions. We consider the production of excited electrons with spin-1/2 at the future SPPC-based electron-proton colliders with center-of-mass energies of 8.44, 11.66, 26.68 and 36.88 TeV. In the  $ep \rightarrow e^*X \rightarrow e\gamma X$  signal process, excited electrons are produced by contact interactions and decay into the photon channel by gauge interactions. Taking into account the corresponding background process, the pseudorapidity and transverse momentum distributions of the final state particles are plotted. We reported the discovery, observation and exclusion mass limits of excited electrons by applying appropriate kinematical cuts best suited for amplify the signal of the excited electron signature. We also investigated the highest achievable values of the compositeness scale for the discovery of excited electrons at these colliders.

---

\*Electronic address: [acaliskan@gumushane.edu.tr](mailto:acaliskan@gumushane.edu.tr)

## I. INTRODUCTION

The Standard Model (SM) in particle physics is a fundamental theory that successfully describes the basic particles and three of the four fundamental interactions between these particles. In 2012, the discovery of the Higgs boson at CERN by the ATLAS [1] and CMS [2] detectors confirmed the Electroweak Symmetry Breaking mechanism proposed by the SM. With this discovery, which is a milestone in particle physics, the mechanism of gaining mass to particles has been experimentally proven. Although all the experiments performed so far have confirmed the SM, there are many phenomena that this theory has not yet been able to explain, such as dark matter, dark energy, elementary particle inflation, family replication and CP violation. In order to provide a theoretical solution to these problems, various theories such as Technicolour [3, 4], Grand Unified Models [5, 6], Supersymmetry [7], Extra Dimensions and Compositeness [8] have been proposed. This study has been conducted within the scope of compositeness theory, as the compositeness can provide a particularly good explanation for fundamental particle inflation. In these models, the existence of more fundamental particles called preons has been proposed. All fermions and their anti-particles are composed of bound states of the preons. The first studies on the lepton and quark compositeness began in the 1970s [9–12]. Up to date, numerous preonic models such as Haplon (Fritzsch-Mandelbaum) [13, 14] and Rishon (Harari-Shupe) [15, 16] have been proposed, suggesting new particles like excited fermions, leptogluons, and leptoquarks within the scope of these models. According to preonic models, possible new interactions between fermions occur on the binding energy scale of the preons. This energy scale, where preons come together to form SM fermions, is called the compositeness scale and is denoted by  $\Lambda$ . If the leptons and quarks in the SM have a composite structure, their excited states should be observed experimentally as a requirement of compositeness. Therefore, excited leptons and quarks are among the proposed new particles. The masses of these proposed particles are expected to be heavier than their SM counterparts.

In the literature, many studies on excited leptons [17][18][19][20][21][22] and quarks [23][24][25] have been carried out for various colliders. In this study, single production of excited electron by contact interaction method is investigated. It is a continuation of our previous work [26] in which the production by gauge mechanism was investigated. No signal for the existence of excited leptons has been found in experimental studies. However, each

new study updates the experimental mass limits of excited leptons. The most recent mass limits for single production of excited electrons are 3.9 TeV for gauge decay [27, 28] and 5.6 TeV for contact decay [29]. Since the decay of excited electrons by gauge interactions is considered in this study, the mass limit of 3.9 TeV is taken into account. This mass limit is provided by the CMS detector for the process  $pp \rightarrow ee^*X \rightarrow ee\gamma X$ , assuming  $f = f' = 1$  and  $\Lambda = m_{e^*}$ .

In this study, the production of excited electrons by contact interactions and their decay by the gauge mechanism were investigated in the SPPC-based electron-proton colliders, which is proposed to be established in China. The rest of the paper is organised as follows: the second section describes the SPPC-CEPC project and the proposed electron-proton collider options, the third section discusses the Lagrangian, decay width and cross sections of excited leptons, the fourth section performs the signal-background analysis and the last section interprets the results obtained.

## II. THE SPPC PROJECT AND ELECTRON - PROTON COLLIDERS

Particle physics has reached the Higgs era with the definitive proof of the existence of the Higgs particle in experiments conducted at CERN. In order to further our knowledge on this subject, the properties of the Higgs particle need to be analysed in more detail. For this purpose, efforts to establish Higgs factories to produce the Higgs particle at higher energies have been initiated all over the world. Thanks to the Higgs factories, more information about the Higgs field will be obtained by carrying out studies on topics such as the precise measurement of the Higgs mass and the observation of rare decay products. Studies on new particles and interactions beyond the SM will also be carried out at these factories.

Just a few months after the discovery of the Higgs particle, the Chinese Particle Physics Community proposed the two-stage CEPC-SPPC project. In the first phase of the project, an electron-positron collider named Circular Electron Positron Collider (CEPC) will be installed. The CEPC collider to be built in China will have a tunnel length of approximately 100 km, where electron and positron beams travelling in opposite directions will be collided in detectors to be installed at two points [30, 31]. The center-of-mass energies of the collider are targeted to be 91, 160 and 240 GeV with corresponding luminosities of 32, 10 and  $3 \times 10^{34} \text{cm}^{-2} \text{s}^{-1}$ , respectively. Since the main purpose of the collider is to investigate the

properties of the Higgs particle, it will work as a Higgs factory for the first 7 years and it is expected to produce at least 1 million Higgs particles during this process. In the following times, it is planned to produce 1 trillion  $Z$  bosons in 2 years as a super  $Z$  factory and 100 million  $W$  bosons in 1 year as a  $W$  factory. In the second phase of the project, a proton-proton collider, the Super Proton Proton Collider (SPPC), will be built as an energy frontier and a discovery machine beyond the LHC [32].

At the SPPC collider, which will share the same tunnel with the CEPC collider, it will be tried to reach a center-of-mass energy of 70 – 75 TeV with dipole magnets of 12 T in the first stage. The SPPC, which is expected to reach a luminosity of  $1 \times 10^{35} \text{ cm}^{-2} \text{ s}^{-1}$ , will be a more powerful  $pp$  collider than the LHC at CERN with these values. At the next stage of the project, it is planned to increase the center-of-mass energy of the SPPC collider to energies of 125 – 150 TeV by using a 20 T dipole magnets. With these energy values, the SPPC collider will be more powerful than the 100 TeV  $pp$  collider in the FCC project [33–36]. The SPPC collider is planned to be installed after 2040 [37]. The Preliminary Content Design Report (Pre-CDR) of the CEPC-SPPC project was written in 2015 [38] and the Content Design Report (CDR) in 2018 [39, 40]. The Technical Design Report (TDR) of the project is still in progress and is expected to be finalised in the coming months.

The installation of the CEPC and SPPC colliders in the same tunnel will enable the  $ep$  collision option in addition to  $pp$  and  $ee^+$  collisions. As a result of a preliminary study on this subject, parameters  $\sqrt{s} = 4.1 \text{ TeV}$  and  $L_{ep} = 10^{33} \text{ cm}^{-2} \text{ s}^{-1}$  were obtained [41]. It can be seen that the center-of-mass energy is quite small here. Because, the problem of synchrotron radiation in circular electron accelerators prevents reaching high energies. If a linear electron accelerator is used instead of a circular one, an  $ep$  collider with a higher center-of-mass energy can be obtained. In another study in this direction, a linear electron accelerator tangential to the SPPC proton ring was proposed and the basic parameters for the  $ep$  option were derived [42]. Higher center-of-mass energies were achieved in this study, which used the parameters of the ILC and PWFALC linear electron accelerator projects as the electron source. For the proton energy, two options were used: 35.6 TeV, an energy value that can be reached in the first stage of SPPC, and 68 TeV, that can be reached in the second stage. Thus, four different  $ep$  collision options were derived. These parameters are given in Table 1.

Table I: The main parameters of the SPPC - based electron - proton colliders.

$E_e(TeV)$	$E_p(TeV)$	$\sqrt{s} (TeV)$	$L_{int} (cm^{-2}s^{-1})$
0.5	35.6	8.44	$2.51 \times 10^{31}$
0.5	68	11.66	$6.45 \times 10^{31}$
5	35.6	26.68	$7.37 \times 10^{30}$
5	68	36.88	$1.89 \times 10^{31}$

### III. GAUGE AND CONTACT INTERACTIONS FOR EXCITED ELECTRONS

Both the production and decay processes of excited leptons in colliders can take place by two different interaction mechanisms. If the interaction between particles is realised by the exchange of specific particles, this interaction is defined as a gauge interaction. The gauge interaction Lagrangian between spin-1/2 excited leptons, ordinary leptons and gauge bosons is given in Equation 1 [43, 44].

$$L_G = \frac{1}{2\Lambda} \bar{L}_R^* \sigma^{\mu\nu} [fg \frac{\vec{\tau}}{2} \cdot \vec{W}_{\mu\nu} + f'g' \frac{Y}{2} B_{\mu\nu}] L_L + h.c., \quad (1)$$

where  $L_L$  and  $L_R^*$  denote left-handed ordinary lepton and right-handed excited lepton, respectively,  $\vec{W}_{\mu\nu}$  and  $B_{\mu\nu}$  are the field strength tensors,  $\Lambda$  is the compositeness scale,  $f$  and  $f'$  are the scaling factors,  $g$  and  $g'$  are the gauge couplings,  $Y$  is hypercharge,  $\sigma^{\mu\nu} = i(\gamma^\mu\gamma^\nu - \gamma^\nu\gamma^\mu)/2$  where  $\gamma^\mu$  are the Dirac matrices, and  $\vec{\tau}$  represents the Pauli matrices.

The other interaction mechanism of excited leptons is four-fermion contact interactions which are effective at short distances. The effective Lagrangian describing this interaction is given in Equation 2 [43, 44].

$$L_C = \frac{g_*^2}{\Lambda^2} \frac{1}{2} j^\mu j_\mu, \quad (2)$$

$$j_\mu = \eta_L \bar{f}_L \gamma_\mu f_L + \eta'_L \bar{f}_L^* \gamma_\mu f_L^* + \eta''_L \bar{f}_L^* \gamma_\mu f_L + h.c. + (L \rightarrow R) \quad (3)$$

In Equations 2 and 3,  $g_*$  is the interaction constant and its value is  $g_*^2 = 4\pi$ .  $\Lambda$  is the compositeness scale and  $j_\mu$  represents the left-handed currents.  $\eta$  factors are the coefficients of these left-handed currents and their value is taken as 1.  $f$  and  $f^*$  are the SM and the excited fermion fields, respectively.

When we analyse both Lagrangians, it is seen that the compositeness scale,  $\Lambda$  is inversely proportional. Therefore, it is clearly seen that as the  $\Lambda$  increases for both interactions, the cross section and decay width values will decrease. However, while the Lagrangians is inversely proportional to  $\Lambda$  in the gauge interaction, it is inversely proportional to  $\Lambda^2$  in the contact interaction. This means that gauge interactions dominate at high  $\Lambda$  values and contact interactions dominate at low  $\Lambda$  values. In this study, since the excited electrons will be produced with the process  $e, p \rightarrow e^*, j$  by the contact interaction method, we set  $\Lambda$  equal to the mass of the excited electron,  $\Lambda = m_{e^*}$ . Thus, we obtained both a high cross section and a situation in which the contact interaction is dominant.

Excited electrons can decay by both mechanisms. There are three decay modes for gauge interactions. These are  $e^* \rightarrow e\gamma$ ,  $e^* \rightarrow eZ$  and  $e^* \rightarrow \nu W^-$  decay channels. If we neglect the SM quark masses and for the  $m^* > m_{W,Z}$  condition, the analytical formulae giving the decay width of these channels are given in Equations 4 below.

$$\Gamma(l^* \rightarrow lV) = \frac{\alpha m^{*3}}{4\Lambda^2} f_V^2 \left(1 - \frac{m_V^2}{m^{*2}}\right)^2 \left(1 + \frac{m_V^2}{2m^{*2}}\right), \quad (4)$$

where  $V$  represents the  $\gamma$ ,  $Z$  and  $W^\pm$  bosons.  $m^*$  is the mass of the excited electron and  $m_v$  is the mass of the gauge boson.  $f_V$  is the interaction constant and its expression for each decay channel is given in Equation 5 below.

$$f_\gamma = fT_3 + f' \frac{Y}{2}$$

$$f_Z = fT_3 \cos^2 \theta_W - f' \frac{Y}{2} \sin^2 \theta_W, \quad (5)$$

$$f_W = \frac{f}{\sqrt{2}}$$

where  $T_3$  is the third component of the weak isospin and  $Y$  is the hypercharge. For excited electrons,  $T_3 = -\frac{1}{2}$  and  $Y = -1$ .  $\theta_W$  is the weak mixing angle.

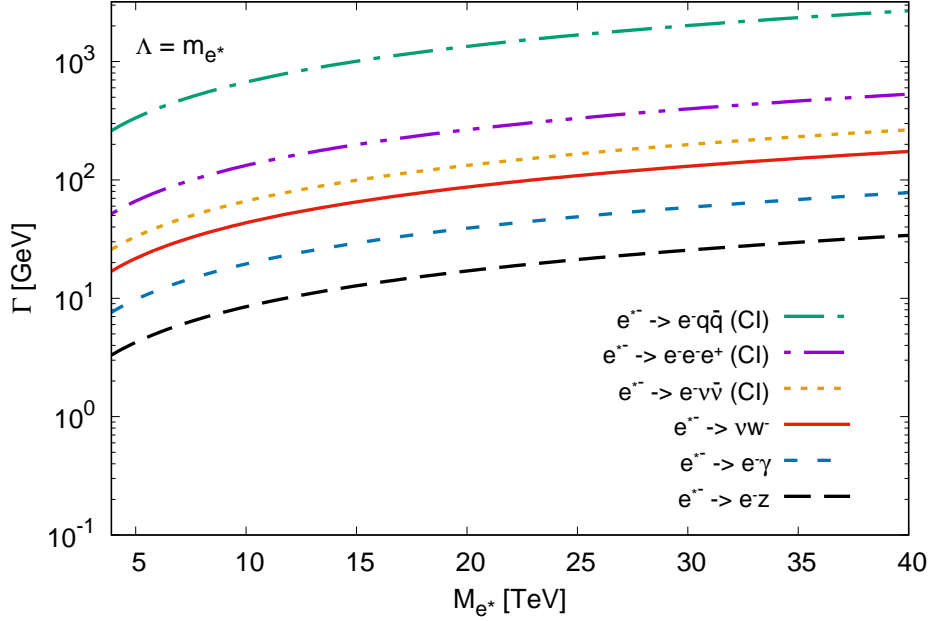


Figure 1: The partial decay widths for both gauge and contact interactions of the excited electron for the energy scale  $\Lambda = m_{e^*}$

Three decay channels are also available for contact interactions. These are the  $e^* \rightarrow eq\bar{q}$ ,  $e^* \rightarrow e^-e^-e^+$  and  $e^* \rightarrow e\nu\bar{\nu}$  processes, where q represents quarks. The analytical formula for the decay width of these processes is given in Equation 6.

$$\Gamma(l^* \rightarrow lF\bar{F}) = \frac{m_l^*}{96\pi} \left(\frac{m_l^*}{\Lambda}\right)^4 N'_C S', \quad (6)$$

In this Equation,  $F$  and  $l$  represent SM fermions and leptons, respectively.  $N'_C$  is the color factor and has a value of 1 for leptons and 3 for quarks.  $S'$  is an additional combinatorical factor with a value of 1 if  $f \neq l$ , 4/3 for quarks and 2 for leptons if  $f = l$ .

For numerical calculations, we implemented both Lagrangians given in Equations 1 and 2 to the CalcHEP simulation package [45] with the help of LanHEP code [46], and created the model file for excited electrons. Since we will use the case where  $\Lambda$  is equal to  $m_{e^*}$  in this study, we calculated the partial decay widths of both interactions for  $\Lambda = m_{e^*}$ . The results are shown in Figure 1.

When this graph is analysed, it is clearly seen that the decay channels of the contact interaction are dominant. The  $eq\bar{q}$  channel has the highest decay width values. If we take each of these decay channels and decay the heavy mass W and Z bosons in the final state,

we obtain the following 6 possible processes for the ep collider.

$$e^- p^+ \rightarrow e^* p \rightarrow e^- q \bar{q} j \quad (7)$$

$$e^- p^+ \rightarrow e^* p \rightarrow e^- e^- e^+ j \quad (8)$$

$$e^- p^+ \rightarrow e^* p \rightarrow e^- \nu \bar{\nu} j \quad (9)$$

$$e^- p^+ \rightarrow e^* p \rightarrow W^- \nu j \rightarrow e^- \bar{\nu} \nu j \quad (10)$$

$$e^- p^+ \rightarrow e^* p \rightarrow e^- \gamma j \quad (11)$$

$$e^- p^+ \rightarrow e^* p \rightarrow e^- Z j \rightarrow e^- q \bar{q} j (e^- e^- e^+ j) \quad (12)$$

Since the photon channel has fewer final state particles and is easier to observe in the detector, we chose this channel for this study. In addition, the photon channel was also used in the last experimental study conducted by the CMS group, where the most recent mass limits of excited leptons were determined. In this experimental study, excited leptons were produced by contact interactions and decayed by gauge interactions and the photon channel was chosen. Therefore, in this paper, we have taken exactly this experimental work as an example. In addition to the mass limits, the CMS group also obtained the most recent compositeness scale limit. For a 1 TeV excited lepton mass, the compositeness scale is excluded up to 25 TeV.

After selecting the photon decay channel, the cross section values of the  $ep \rightarrow e\gamma j$  process for the proposed 4 ep collider options were calculated for  $\Lambda = m_{e^*}$  and the results are shown in Figure 2. As seen in these graphs, excited electrons are produced for both interactions and then decayed into the photon channel. Thus, we have compared both production mechanisms in these graphs. As it is clearly seen in all graphs, contact production dominates over gauge production for the  $\Lambda = m_{e^*}$  condition. On the other hand, considering the luminosity values in Table 1, these four colliders have the capacity to produce a sufficient number of events.



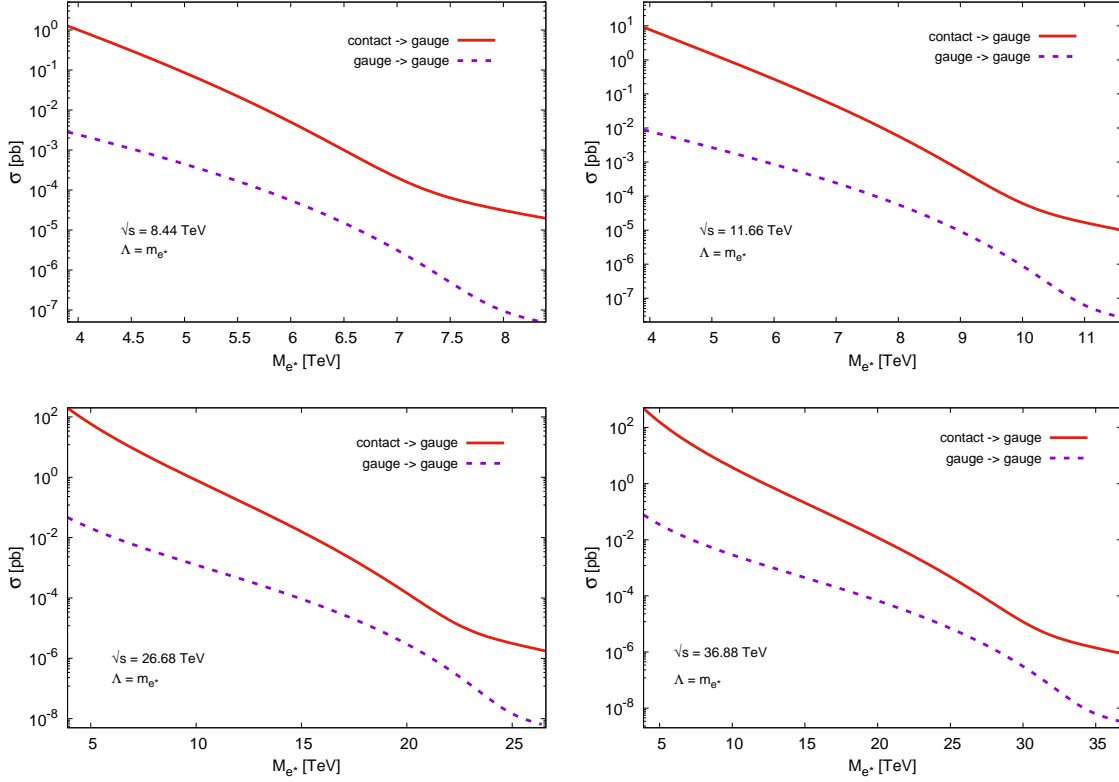


Figure 2: The cross-sections of the excited electrons for both production mechanism with respect to its mass at the SPPC-based electron-proton colliders with various center-of-mass energies for  $\Lambda = m_{e^*}$  and the coupling  $f = f' = 1$ .

#### IV. SIGNAL AND BACKGROUND ANALYSIS

The SPPC-based  $ep$  colliders will enable us to search for excited electrons through the process  $ep \rightarrow e^*j$  (contact interaction), followed by the subsequent decay of the excited electrons into an electron and photon (gauge decay). Therefore, our signal process is  $ep \rightarrow e, \gamma, j$ , where  $j$  represents jets and consists of quarks and antiquarks. The subprocesses of our signal are of the form  $eq(\bar{q}) \rightarrow e\gamma q(\bar{q})$ , where  $q$  represents quarks and  $\bar{q}$  represents antiquarks. The Feynman diagram of our signal process is shown in Figure 3.

The main background process corresponding to our signal is  $ep \rightarrow e, \gamma, j$ . Other complex SM processes are not considered here, because their contribution would be too small.

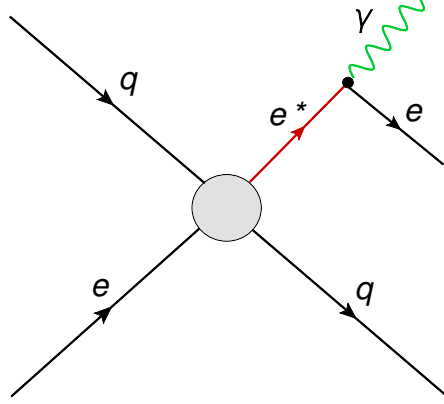


Figure 3: Leading-order Feynman diagrams for the signal process  $ep \rightarrow e, \gamma, j$ .

### Detector Parameters

Since a detailed detector design for SPPC-based ep colliders has not yet been carried out, the signal-background analysis is performed at the parton level. However, in this subsection, the sensitivity of today’s detector technology in the measurement of some basic parameters will be briefly discussed. For this purpose, the parameters of the ATLAS detector of the High Luminosity LHC (HL-LHC) project [47], which is planned to be commissioned in 2029, are considered. The ATLAS detector is being upgraded to suit the operating conditions of the HL-LHC. For this purpose, the detector’s Inner Tracker system will be completely replaced with a new silicon-only design. In this way, it is aimed to achieve higher momentum resolution. In addition, the pseudorapidity values, which express the tracking range of the detector, will be extended from  $|\eta| < 2.5$  to  $|\eta| < 4$ .

In this study, the final state particles of our signal and background process are electrons, photons and jets. Some important detector parameters of these particles are reconstruction, identification, isolation efficiency, energy scale and momentum resolution. The systematic uncertainties to be achieved at HL-LHC for these parameters are given in Table 2 [48].

According to the data in this table, it is understood that very high precision measurements can be made. In a future ep detector, with the further development of technology, much more sensitive measurements will be possible.

Table II: Representative systematic uncertainties in the measurement of some parameters of electron, photon and jets at the HL-LHC.

Particles	Parameters	Range	Uncertainty (%)
Electron	Energy Scale	$P_T \approx 45\text{GeV}$	0.1
	Energy Scale	up to 200 GeV	0.3
	Reconstruction+Identification Efficiency (ID)	$P_T \approx 45\text{GeV}$	0.5
	Reconstruction+ID+Isolation Efficiency	$P_T > 200\text{GeV}$	2
Photon	Energy Scale	$P_T \approx 60\text{GeV}$	0.3
	Energy Scale	up to 200 GeV	0.5
	Resolution	$P_T \approx 60\text{GeV}$	10
	Reconstruction+ID+Isolation Efficiency	$P_T < 200\text{GeV}$	2
Jets	Absolute Jet Energy Scale	-	1 – 2
	Pileup	-	0 – 2
	Jet Flavour Composition	-	0 – 0.5
	Jet Flavour Response	-	0 – 0.8
	b-jet efficiency	$30 < P_T < 300 \text{ GeV}$	1
	b-jet efficiency	$P_T > 300 \text{ GeV}$	2 – 6
	c-jet efficiency	all working points	2
	light-jet mistag	working-point dependent	5 – 15

### Kinematical Cuts For Discovery Of Excited Electrons

In the signal-background analysis, we first applied pre-selection cuts  $P_T^{e,\gamma,j} > 25 \text{ GeV}$  to the transverse momentum of the final state particles, electron, photon and jet in order to separate the excited electron signals from the background. We then obtained some kinematic distributions for both signal and background and superimposed them on the same graph, so that we could compare signal and background. First, transverse momentum ( $P_T$ ) and pseudorapidity ( $\eta$ ) distributions for the final state particles, electrons, photons and jets, of the ep collider with a center-of-mass energy of 8.44 TeV are plotted. In these distributions, mass values of  $m_{e^*} = 3900, 5000, 6000, 7000 \text{ GeV}$  were used for the signal. Since the  $P_T$  and  $\eta$  distributions of the electron and photon are similar, only the distributions of the electron

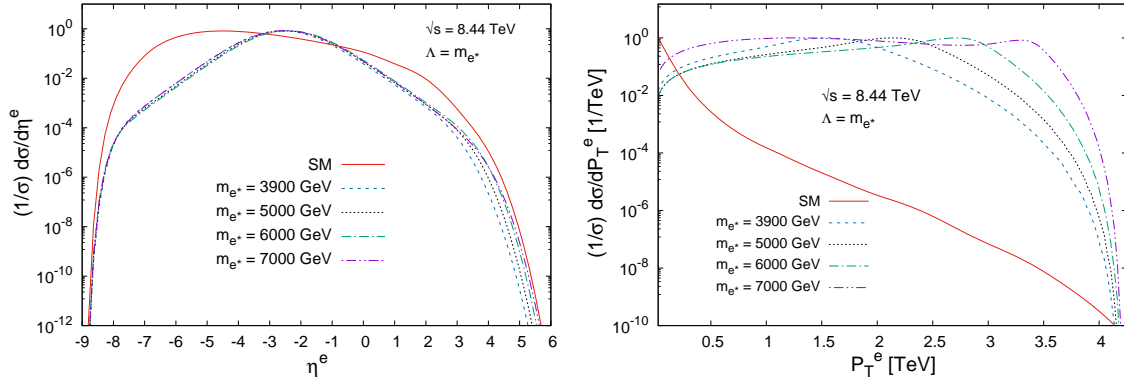


Figure 4: The normalized pseudorapidity (left) and transverse momentum (right) distributions of the final state electrons for the ep collider with center-of- mass energy 8.44 TeV.

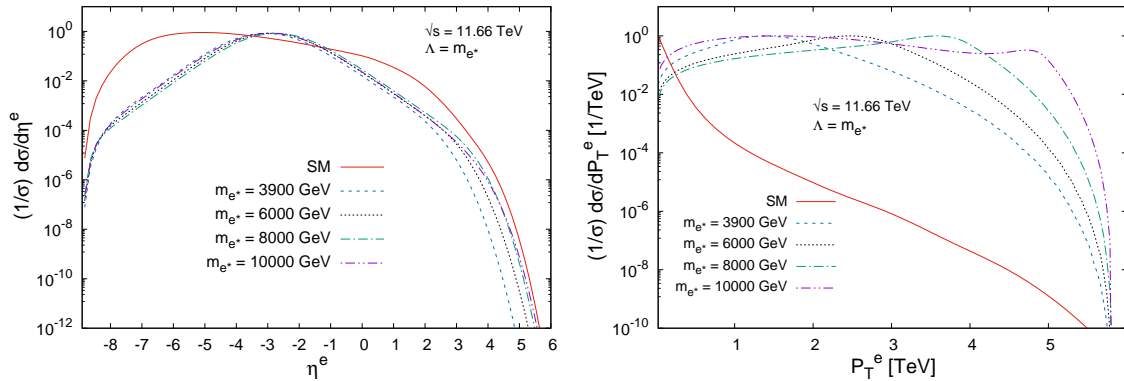


Figure 5: The normalized pseudorapidity (left) and transverse momentum (right) distributions of the final state electrons for the ep collider with center-of- mass energy 11.66 TeV.

are given and these are shown in Figure 4.

Similar procedures were performed for the other ep colliders with center-of-mass energies of 11.66, 26.68 and 36.88 TeV and the resulting distributions are shown in Figure 5, Figure 6 and Figure 7, respectively.

When we examine the pseudorapidity plots of the final state particles, it is clearly seen that these distributions peak in the negative region at all ep colliders. Considering that pseudorapidity is mathematically defined as  $\eta = -\ln \tan(\theta/2)$ , where  $\theta$  is polar angle, it is understood that electrons and photons are spatially backward, so we can say that excited electrons are mostly produced in the backward direction. This is mainly due to the asymmetric nature of the ep colliders. Since the energy of the electron is smaller, the

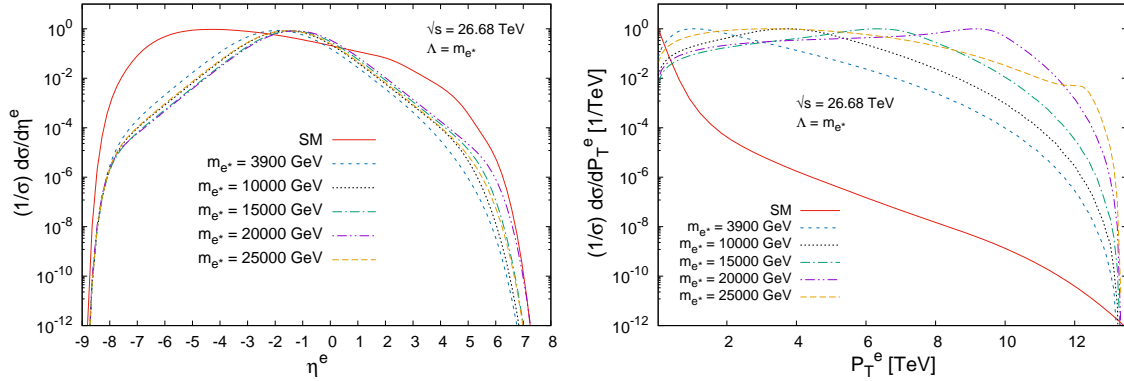


Figure 6: The normalized pseudorapidity (left) and transverse momentum (right) distributions of the final state electrons for the ep collider with centre-of- mass energy 26.68 TeV.

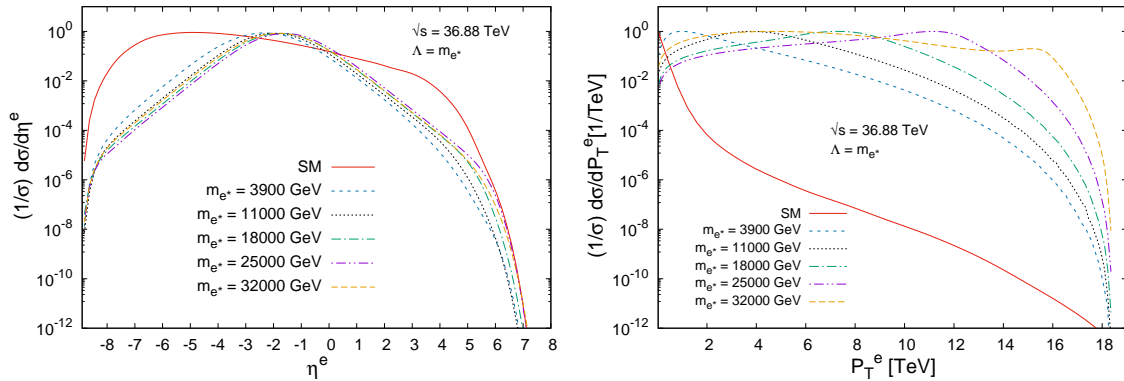


Figure 7: The normalized pseudorapidity (left) and transverse momentum (right) distributions of the final state electrons for the ep collider with centre-of- mass energy 36.88 TeV.

pseudorapidity distributions are boosted towards the side from which the electron beam comes. Therefore, they peaked in the negative region.

On the other hand, when all  $P_T$  and  $\eta$  plots are analysed, it is seen that the signal and background distributions are slightly separated from each other. However, since the cross section of the background is larger, this separation is not sufficient to identify the signal from the background. Therefore, in addition to the pre-selection cuts, we need to apply large cuts, so-called discovery cuts. If we select regions  $-3.5 < \eta^e < -0.5$  in the  $\eta$  plot and  $p_T^e > 500$  GeV in the  $P_T$  plots in Figure 4, these cuts will hardly change the cross section of the signal. On the other hand, they will dramatically reduce the cross section of the background. A similar method was followed for the other  $P_T$  and  $\eta$  distributions, i.e.

Table III: The discovery cuts in the  $P_T$  and  $\eta$  distributions of final state particles at SPPC-based ep colliders.

$\sqrt{s}$ [TeV]	$p_T^e$	$p_T^\gamma$	$p_T^j$	$\eta^e$	$\eta^\gamma$	$\eta^j$
8.44	$p_T^e > 500$ GeV	$p_T^\gamma > 500$ GeV	$p_T^j > 500$ GeV	$-3.5 < \eta^e < -0.5$	$-3.5 < \eta^\gamma < -0.5$	$-4 < \eta^j < 2.5$
11.66	$p_T^e > 500$ GeV	$p_T^\gamma > 500$ GeV	$p_T^j > 500$ GeV	$-3.5 < \eta^e < -1$	$-3.5 < \eta^\gamma < -1$	$-4 < \eta^j < 2.5$
26.68	$p_T^e > 500$ GeV	$p_T^\gamma > 500$ GeV	$p_T^j > 500$ GeV	$-2.5 < \eta^e < 0.5$	$-2.5 < \eta^\gamma < 0.5$	$-4 < \eta^j < 2.5$
36.88	$p_T^e > 500$ GeV	$p_T^\gamma > 500$ GeV	$p_T^j > 500$ GeV	$-2.5 < \eta^e < 0$	$-2.5 < \eta^\gamma < 0$	$-4 < \eta^j < 2.5$

discovery cuts were determined so as not to affect the signal too much and to reduce the background. Determined discovery cuts for the  $P_T$  and  $\eta$  distributions of the particles of electron, photon and jet in the final state are reported in Table 3. This table also shows the discovery cuts of the jets. But, their distribution plots are not given in this paper since the jets are not directly related to our signal.

One of the most powerful methods to separate the signal from the background is to apply a cut to the electron-photon invariant mass distributions. The invariant mass distribution plots obtained after applying pre-selection cuts are shown in Figure 8. In these plots, it can be seen that the line belonging to the background distribution is below the signal peaks. If we apply an invariant mass cut in the form  $m_{e^*} - 2\Gamma_{e^*} < m_{e\gamma} < m_{e^*} + 2\Gamma_{e^*}$ , where  $\Gamma$  shows the decay width of excited electron, we can make this line lower. The invariant mass cut is much more effective than the others. So we also applied this effective cut.

In addition to the above mentioned cuts, we applied some separation cuts in order to distinguish the final-state particles from each other. We applied the  $\Delta R(e, \gamma) = 0.7$  [27] cut to separate the electron from the photon and the  $\Delta R(j, \gamma) = \Delta R(j, e) = 0.4$  [29] cuts to separate the jets from the electron and photon. Here  $\Delta R$  is the separation cut and is defined as  $\Delta R = \sqrt{\Delta\eta^2 + \Delta\phi^2}$ .

### Significance Calculus

In the signal-background analysis, the discovery cuts mentioned in the previous subsection were used to separate the signal from the background and the Statistical Significance (SS) values of the expected signal yield were calculated. The following formula was used to

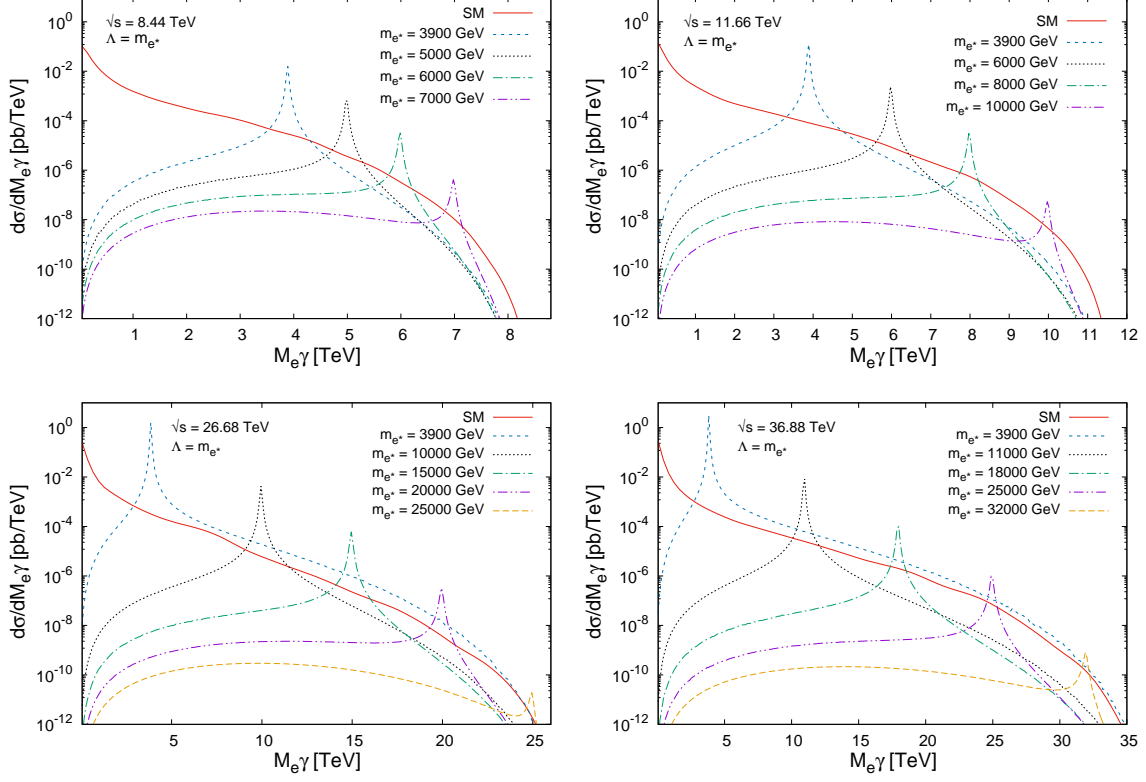


Figure 8: The invariant mass distributions of excited electron and corresponding background for SPPC-based ep colliders.

calculate the SS values [49].

$$SS = \sqrt{2 \left[ (S + B) \ln \left( 1 + \left( \frac{S}{B} \right) \right) - S \right]}, \quad (13)$$

where S and B denote event numbers of the signal and background, respectively. Using the data obtained as a result of the calculations, the variation graphs of the SS with respect to the mass of the excited electron were plotted. SS plots for all colliders are shown in Figure 9.

Afterwards, more detailed calculations were performed to obtain the discovery ( $5\sigma$ ), observation ( $3\sigma$ ) and exclusion ( $2\sigma$ ) values of the mass of the excited electron. According to the findings, the ep collider with a center-of-mass energy of 8.44 TeV will have the potential to discover excited electrons up to mass 5650 GeV, observe them up to mass 5935 GeV and exclude them up to mass 6140 GeV. The mass limits obtained for all colliders are reported in Table 4.

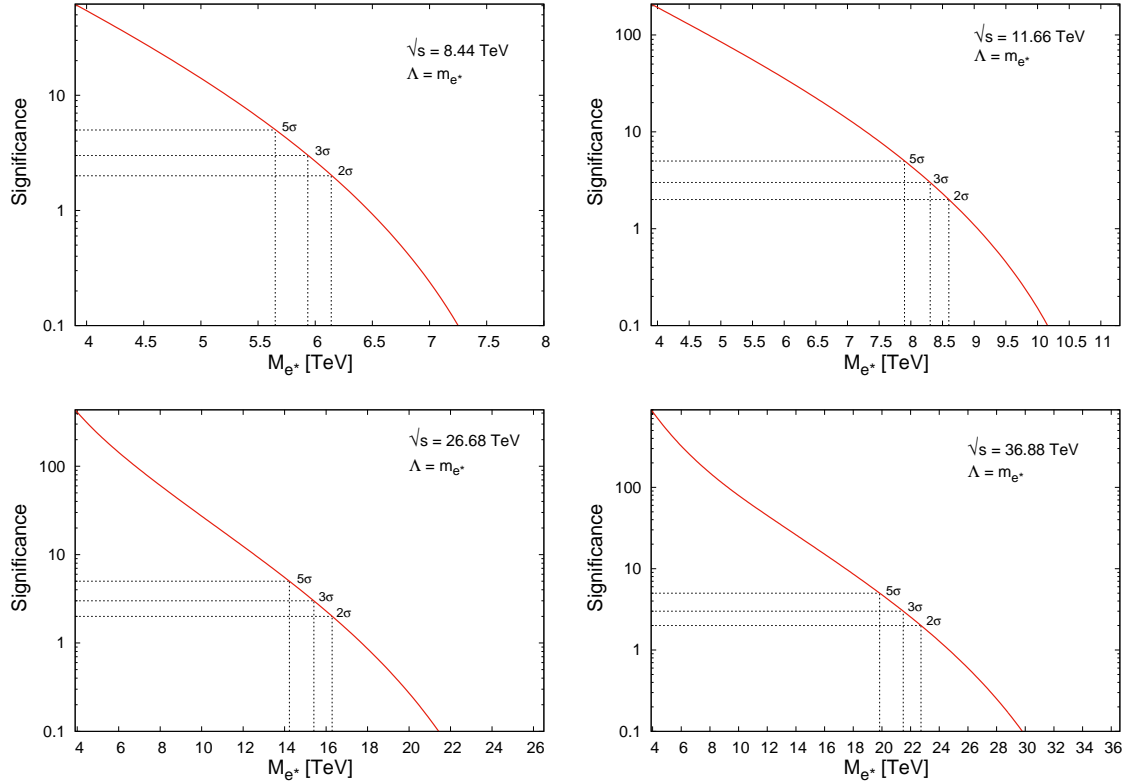


Figure 9: Plots of the variation of statistical significance (SS) with respect to the mass of the excited electron at SPPC-based ep colliders

Table IV: Attainable mass limits of the excited electrons for SPPC-based ep colliders

$\sqrt{s}$ (TeV)	$5\sigma$ (GeV)	$3\sigma$ (GeV)	$2\sigma$ (GeV)
8.44	5650	5935	6140
11.66	7900	8305	8600
26.68	14230	15410	16290
36.88	19840	21485	22725

In addition to these calculations, the highest compositeness scale values that can be achieved for each collider were calculated. The calculations show that as the mass of the excited electron increases, the compositeness scale values decrease inversely. Therefore, in order to reach the highest compositeness scale values, we should look for the smallest mass value. Considering that excited electrons are experimentally excluded up to 3.9 TeV, it would be appropriate to take the mass of the excited electron as 4 TeV for this calculation.



Table V: Attainable compositeness scale limits of the excited electrons with a mass of 4 TeV for SPPC-based ep colliders

$\sqrt{s}$ (TeV)	$5\sigma$ (GeV)	$3\sigma$ (GeV)	$2\sigma$ (GeV)
8.44	11800	14780	17625
11.66	21000	26200	31150
26.68	29830	37215	44210
36.88	41915	52260	62050

Choosing the mass of the excited electron at 4 TeV, the values of the compositeness scale corresponding to  $2\sigma$ ,  $3\sigma$  and  $5\sigma$  were calculated for each ep collider and the results are listed in Table 5. According to these results, the highest compositeness scale value can be reached at the collider with a center-of-mass energy of 36.88 TeV. At this collider, the compositeness scale for the discovery of the excited electron is 41915 GeV.

## V. CONCLUSION

In this study, we investigate the production of excited electrons by contact interactions and their decay into the photon channel by gauge interactions at ep colliders. Calculations were performed for four different SPPC-based electron-proton colliders with center-of-mass energies of 8.44, 11.66, 26.68 and 36.88 TeV. In the signal-background analysis, in addition to pre-selection cuts, discovery cuts were applied to separate the excited electron signal from the background. In all calculations for the signal, the compositeness scale was taken equal to the mass of the excited electron. According to the results, excited electrons can be discovered up to 5650 GeV at a collider with a center-of-mass energy of 8.44 TeV and an integrated luminosity of  $251 \text{ pb}^{-1}$ , and up to 7900 GeV at a collider with a center-of-mass energy of 11.66 TeV and an integrated luminosity of  $645 \text{ pb}^{-1}$ . In the last two high-energy ep colliders, the collider with a center-of-mass energy of 26.68 TeV and an integrated luminosity of  $73.7 \text{ pb}^{-1}$  will be able to discover up to 14230 GeV, and the collider with a center-of-mass energy of 36.88 TeV and an integrated luminosity of  $189 \text{ pb}^{-1}$  will be able to discover up to 19840 GeV.

In the last part of the study, the highest compositeness scale achievable at these colliders

was investigated. Accordingly, excited electrons with a mass of 4 TeV can be discovered up to 11800 GeV at the ep collider with a center of mass energy of 8.44 TeV, 21000 GeV at the collider with a center of mass energy of 11.66 TeV, 29830 GeV at the collider with a center of mass energy of 26.68 TeV and 41915 GeV at the collider with a center of mass energy of 36.88 TeV. All these calculations for excited electrons show that SPPC-based ep colliders will provide the possibility to scan a wide mass range for excited lepton searches. The observation of any excited lepton signal at these colliders will provide direct evidence for the existence of composite models.

### **Conflict of Interest**

The author declares that he has no conflict of interest.

### **Acknowledgments**

I would like to thank Dr. M. Sahin from Usak University, Türkiye, for his support for the model file and for the useful consultations we had.

- 
- [1] ATLAS Collaboration, “Observation of a new particle in the search for the Standard Model Higgs boson with the ATLAS detector at the LHC”, *Phys. Lett. B*, 716 (1), 1-29 (2012).
  - [2] CMS Collaboration, “Observation of a new boson at a mass of 125 GeV with the CMS experiment at the LHC”, *Phys. Lett. B*, 716 (1), 30-61 (2012).
  - [3] S. Weinberg, “Implications of dynamical symmetry breaking”, *Phys. Rev. D*, 13, 974-996 (1976).
  - [4] L. Susskind, “Dynamics of spontaneous symmetry breaking in the Weinberg-Salam theory”, *Phys. Rev. D*, 20, 2619-2625 (1979).
  - [5] H. Georgi and S. L. Glashow, “Unity of all elementary-particle forces”, *Phys. Rev. Lett.*, 32, 438 (1974).
  - [6] J. C. Pati and A. Salam, “Lepton number as the fourth color”, *Phys. Rev. D*, 10, 275 (1974).
  - [7] Y. A. Golfand and E. P. Likhtman, “Extension of the algebra of poincare group generators and violation of P invariance”, *JETP Lett.*, 13, 323 (1971).

- [8] I.A. D'Souza and C.S. Kalman, PREONS: Models of leptons, quarks and gauge bosons as composite objects, World Scientific Publishing, 1992.
- [9] H. Terazawa, Y. Chikashige and K. Akama, "Unified model of the Nambu-Jona-Lasinio type for all elementary-particle forces", *Phys. Rev. D*, 15 (2), 480 (1977).
- [10] H. Terazawa, "Subquark model of leptons and quarks", *Phys. Rev. D*, 22 (1), 184 (1980).
- [11] H. Terazawa, M. Yasue, K. Akama and M. Hayashi, "Observable effects of the possible substructure of lepton and quarks", *Phys. Lett. B*, 112 (4-5), 387-392 (1982).
- [12] H. Terazawa, "A fundamental theory of composite particles and fields", *Phys. Lett. B*, 133 (1-2), 57-60 (1983).
- [13] H. Fritzsch and G. Mandelbaum, "Weak interactions as manifestations of the substructure of leptons and quarks", *Phys. Lett. B*, 102 (5), 319-322 (1981).
- [14] O.W. Greenberg and J. Sucher, "A quantum structure dynamic model of quarks, leptons, weak vector bosons and Higgs mesons", *Phys. Lett. B*, 99 (4), 339-343 (1981).
- [15] H. Harari, "A schematic model of quarks and leptons", *Phys. Lett. B*, 86 (1), 83-86 (1979).
- [16] M.A. Shupe, "A composite model of leptons and quarks", *Phys. Lett. B*, 86 (1), 87-92 (1979).
- [17] M. Sahin and A. Caliskan, "Excited muon production in muon colliders via contact interaction", *Journal of Physics G: Nuclear and Particle Physics*, 50 (2), 025002 (2023).
- [18] A. Caliskan, "Search for excited muons at the future SPPC-based muon-proton colliders", *Acta Physica Polonica B*, 50, 1409-1422 (2019).
- [19] A. Caliskan, S. O. Kara, "Single production of the excited electrons in the future FCC-based lepton-hadron colliders", *International Journal of Modern Physics A*, 33 (24), 1850141 (2018).
- [20] A. Caliskan, "Single production of the excited muons at the SPCC-based ultimate  $\mu p$  collider", *Turkish Journal Physics*, 42 (4), 343-349 (2018).
- [21] A. Caliskan, S.O. Kara and A. Ozansoy, "Excited muon searches at the FCC-based muon-hadron colliders", *Adv. High Energy Phys.*, 2017, 1540243 (2017).
- [22] A. Caliskan, "Excited neutrino search potential of the FCC-based electron-hadron colliders", *Adv. High Energy Phys.*, 2017, 4726050 (2017).
- [23] M. Sahin, G. Aydin and Y. O. Günaydin, "Excited quarks production at FCC and SppC pp Colliders", *International Journal of Modern Physics A*, 34 (29), 1950169 (2019).
- [24] A. N. Akay et al., "Search for excited u and d quarks in dijet final states at future pp colliders", *Advances in High Energy Physics*, 2019, 9090785, 1-11 (2019).

- [25] Y. O. Günaydin, M. Sahin and S. Sultansoy, “Resonance production of excited u quark at FCC-based  $\gamma p$  colliders”, *Acta Physica Polonica B*, 10 (49), 1763-1779 (2018).
- [26] A. Caliskan, “Single production of composite electrons at the future SPPC-based lepton-hadron colliders”, *Canadian Journal of Physics*, 98 (4) (2020).
- [27] The CMS collaboration., Sirunyan, A.M., Tumasyan, A. et al, “Search for excited leptons in  $ll\gamma$  final states in proton-proton collisions at  $\sqrt{s} = 13$  TeV”, *J. High Energ. Phys.* 2019, 15 (2019). [https://doi.org/10.1007/JHEP04\(2019\)015](https://doi.org/10.1007/JHEP04(2019)015).
- [28] R.L. Workman et al., (Particle Data Group), “The review of particle physics”, *Prog. Theor. Exp. Phys.*, 2022, 083C01 (2022).
- [29] The CMS collaboration., Sirunyan, A.M., Tumasyan, A. et al, “Search for an excited lepton that decays via a contact interaction to a lepton and two jets in proton-proton collisions at  $\sqrt{s} = 13$  TeV”, *J. High Energ. Phys.* 2020, 52 (2020). [https://doi.org/10.1007/JHEP05\(2020\)052](https://doi.org/10.1007/JHEP05(2020)052).
- [30] Y. Li, “CEPC Accelerator TDR Status Overview”, ICFA Advanced Beam Dynamics Workshop on High Luminosity Circular  $e^+e^-$  Colliders (65th), JACoW eeFACT2022 14-18, [doi:10.18429/JACoW-eeFACT2022-MOXAT0105](https://doi.org/10.18429/JACoW-eeFACT2022-MOXAT0105), (2023).
- [31] J. Gao, “CEPC Accelerator TDR Status and AC Power Consumptions”, ICFA Advanced Beam Dynamics Workshop on High Luminosity Circular  $e^+e^-$  Colliders (65th), JACoW eeFACT2022 262-269, [doi:10.18429/JACoW-eeFACT2022-FRXAS0102](https://doi.org/10.18429/JACoW-eeFACT2022-FRXAS0102), (2023).
- [32] CEPC Project Web Page: <http://cepc.ihep.ac.cn/intro.html>.
- [33] FCC Collaboration, “Future Circular Collider Study Volume 1: Physics Opportunities”, Conceptual Design Report, *Eur. Phys. J. C*, 79:474 (2019).
- [34] FCC Collaboration, “Future Circular Collider Study Volume 2: The Lepton Collider (FCC-ee)”, Conceptual Design Report, *Eur. Phys. J. ST*, 228:261-623 (2019).
- [35] FCC Collaboration, “Future Circular Collider Study Volume 3: The Hadron Collider (FCC-hh)”, Conceptual Design Report, *Eur. Phys. J. ST*, 228:755-1107 (2019).
- [36] FCC Collaboration, “Future Circular Collider Study Volume 4: The High Energy LHC (HE-LHC)”, Conceptual Design Report, *Eur. Phys. J. ST*, 228:1109-1382 (2019).
- [37] J. Tang, “Design Concept for a Future Super Proton-Proton Collider”, *Frontiers in Physics*, 10:828878 (2022).
- [38] The CEPC-SPPC Study Group, CEPC-SPPC Preliminary Conceptual Design Report, Volume I - Physics & Detector, IHEP-CEPC-DR-2015-01, March (2015).

- [39] CEPC Study Group, “CEPC Conceptual Design Report: Volume 1 - Accelerator”, Conceptual Design Report, IHEP-CEPC-DR-2018-01, IHEP-AC-2018-01, arXiv preprint: 1809.00285 (2018).
- [40] CEPC Study Group, “CEPC Conceptual Design Report: Volume 2 - Physics & Detector”, Conceptual Design Report, HEP-CEPC-DR-2018-02, IHEP-EP-2018-01, IHEP-TH-2018-01, arXiv preprint: 1811.10545 (2018).
- [41] Y. Zhang and Y. Peng, “A high energy e-p/A collider based on CepC-SppC”, 6th International Particle Accelerator Conference, IPAC2015, Richmond, VA, USA (2015).
- [42] A. C. Canbay, U. Kaya, B. Ketenoglu, B. B. Oner and S. Sultansoy, “SppC based energy frontier lepton-hadron colliders: Luminosity and physics”, *Adv. High Energy Phys.*, 2017, 4021493 (2017).
- [43] K. Hagiwara, D. Zeppenfeld and S. Komamiya, “Excited lepton production at LEP and HERA”, *Z. Phys. C*, 29, 115 (1985).
- [44] U. Baur, M. Spira and P. M. Zerwas, “Excited-quark and -lepton production at hadron colliders”, *Phys. Rev. D*, 42 (3), 815 (1990).
- [45] A. Belyayev, N. D. Christensen and A. Pukhov, “CalcHEP 3.4 for collider physics within and beyond the Standard Model”, *Comput. Phys. Commun.*, 184, 1729 (2013).
- [46] A. Semenov, “LanHEP - A package for automatic generation of Feynman rules from the Lagrangian. Version 3.2,”, *Comput. Phys. Commun.*, 201, 167-170 (2016).
- [47] O. Aberle, C. Adorisio, A. Adraktas et al., “High-Luminosity Large Hadron Collider (HL-LHC) Technical Design Report”, CERN Yellow Reports : Monographs, ISSN 2519-8076 (Online), <https://doi.org/10.23731/CYRM-2020-0010>, CERN-2020-010, Switzerland (2010).
- [48] The ATLAS Collaboration, “Expected performance of the ATLAS detector at the High-Luminosity LHC” ATLAS Pub Note, ATL-Phys-PUB-2019-005, <https://inspirehep.net/files/f8aa0be3b939950fdb4a533bb38c8074> (2019).
- [49] G. Cowan, K. Cranmer, E. Gross and O. Vitells, “Asymptotic formulae for likelihood-based tests of new physics”, *The European Physical Journal C*, 71:1554 (2011).